Supplementary information

Nano zero-valent iron aging interacts with soil microbial community: a microcosm study

Songlin Wu[†,*], Tomáš Cajthaml[‡,§], Jaroslav Semerád[‡,§], Alena Filipová[‡], Mariana Klementová[#], Roman Skála[‖,⊥], Martina Vítková[†], Zuzana Michálková[†], Manuel Teodoro[†], Zhaoxiang Wu[¶], Domingo Martínez-Fernández[†], Michael Komárek[†]

[†]Department of Environmental Geosciences, Faculty of Environmental Sciences, Czech University of Life Sciences Prague, Kamýcká 129, 165 00 Prague - Suchdol, Czech Republic

[‡]Institute of Microbiology of the Czech Academy of Sciences, Vídeňská 1083, 142 20 Prague 4, Czech Republic

[§]Institute for Environmental Studies, Faculty of Science, Charles University in Prague, Benátská 2, 128 01 Prague 2, Czech Republic

[#]Institute of Physics of the Czech Academy of Sciences, Na Slovance 2, 182 21 Prague 8, Czech Republic

[‖]Institute of Geology of the Czech Academy of Sciences, Rozvojová 269, 165 00 Prague - Suchdol, Czech Republic

[⊥]Institute of Geochemistry, Mineralogy and Mineral Resources, Faculty of Science, Charles University in Prague, Albertov 6, 128 43 Prague 2, Czech Republic

[¶]Jiangxi Engineering and Technology Research Center for Ecological Remediation of Heavy metal pollution, Institute of Biological Resources, Jiangxi Academy of Sciences, Nanchang 330096, China

*Corresponding author, E-mail address: wusonglin11@gmail.com (Songlin Wu)

This SI contains 27 pages, 8 tables and 14 figures, as well as some experimental methods description.

SEM, TEM/SAED, XRD, ATR-FTIR and Raman analysis

The lyophilized nZVI particles and their aging products were put on carbon conductive tapes and analyzed via scanning electron microscopy (SEM; TESCAN Brno, Czech Republic) with electron dispersive X-ray spectroscopy (EDX; 125 eV, Bruker Nano, Berlin, Germany) in the Institute of Geology of the Czech Academy of Sciences to detect morphological changes during nZVI aging.

For TEM/SAED, powder samples were dispersed in ethanol and the suspension was treated ultrasonically for 5 min. Transmission electron microscopy (TEM) was carried out using an FEI Tecnai TF20 (Massachusetts, USA) X-twin microscope operated at 200 kV (FEG, 1.9Å point resolution) with an EDAX Energy Dispersive X-ray (EDX) detector attached. Images were recorded by a CCD camera with resolution of 2048×2048 pixels using the Digital Micrograph software package. Electron diffraction patterns were evaluated using the Process Diffraction software package.[1]

The lyophilized nZVI aging products were ground into fine powder for XRD, ATR-FTIR and Raman analysis. XRD analysis was conducted using a Bruker D8 Discover diffractometer coupled with a Johansson-type focusing Ge primary monochromator (Bruker, Germany) and a linear silicon strip detector LYNXEYE. The detector was open to 2.896° during the data acquisition. The long-line fine-focus Cu tube was operated at 40 kV and 40 mA (Cu $K_{\alpha 1}$ radiation (1.54056 Å)). The XRD data were collected between 5 and 70° with a step of 0.017°. A counting time of 74 s per a single detector channel was used for all samples. The Bruker software DIFFRAC.EVA (version 4.2) with an ICDD PDF2 database (version 2011) was used for mineral identification. ATR-FTIR spectra were collected between 400 and 4000 cm^{-1} with a resolution of 2 cm^{-1} and 64 scans. Spectra were processed by MicroLab software package and Origin 8.5 (OriginLab Corporation, Northampton, Massachusetts, USA). The Raman spectra were collected with a Spectroscopy & Imaging (S&I) MonoVista CRS+ micro-spectrometer (S&I MonoVista CRS+, Germany). The system is based on an Olympus BX-51 WI upright microscope, Princeton Instruments SpectraPro SP2750 spectrometer (750 mm focal length and aperture ratio f/9.7), and a CCD detector ANDOR iDus 416 with 2000×256 pixels (pixel size 15 µm). A diode-pumped solid-state 532 nm laser (Cobolt Samba) with output of 100 mW attenuated to 3 mW on the sample measured with a power meter was used for spectra excitation. The laser was directed at samples with a 50× magnifying LWD objective. The grating density was 1200 gr/mm. The system was calibrated to the excitation laser line position and silicon and polystyrene standards. Typically, three spectra were collected from each sample within two spectral ranges: 100–1800 cm^{-1} and 3250–3925 cm^{-1}. The software Crystal Sleuth[2] was used to evaluate the spectra.

Phospholipid fatty acid (PLFA) analysis

Phospholipid fatty acid (PLFA) analysis was performed using freeze-dried soil samples. The samples were extracted in triplicate using a mixture of chloroform, methanol, and phosphate buffer (1:2:0.8; v/v/v), transmethylated and analyzed using tandem gas chromatography-mass spectrometry (GC-MS; 450-GC, 240-MS Varian, Walnut Creek, CA, USA); and processed as described by Covino et al. (2016).[3]

Table S1. Basic physico-chemical characteristics of the metal(loid) contaminated soil used in the present microcosm study. Metal(loid) concentration and speciation in the soil were included. Note: Acid-extractable metal(loid)s were extracted by 0.11 mol L^{-1} acetic acid; reducible metal(loid)s were extracted by 0.5 mol L^{-1} hydroxylammonium chloride; and oxidizable metal(loid)s were extracted by 1.0 mol L^{-1} ammonium acetate after being digested using 30% (w/w) hydrogen peroxide. The soil was also separately extracted by 0.01 mol L^{-1} $CaCl_2$ and 0.1 mol L^{-1} EDTA. Concentrations of all metal(loid) species were determined by inductively coupled plasma-optical emission spectrometry (ICP-OES). From Wu et al. (2018).[4]

Property	pH (soil: water=1:2.5)	pH_{zpc} (solid: solution=1:40)	CEC (cmol kg^{-1})	Soil organic matter (g kg^{-1})	Extractable P (mg kg^{-1})	Eh (mV)
Investigated soil	5.95	5.45	9.08	21.5	1.53	426
Metal concentration (mg kg^{-1})	Total	Acid extractable	Reducible	Oxidizable	$CaCl_2$ extractable	EDTA extractable
Fe	37400	12.4	1690	8.36	0.06	793
Mn	4280	111	240	545	9.3	1410
Zn	4000	167	541	307	440	1660
Cu	68.3	8.08	n.d.	28.5	n.d.	32.9
Pb	3540	207	892	596	0.89	2040
Cd	39.1	21.3	8.44	2.13	7.49	24.6
Cr	61.3	n.d.	n.d.	0.92	n.d.	n.d.
Ni	24.4	1.79	n.d.	n.d.	0.31	1.32
As	296	n.d.	n.d.	2.02	n.d.	5.18

Table S2. Physico-chemistry of bare nZVI, CMC-nZVI and PAA-nZVI. Note: nZVI, nano zero-valent iron; CMC, carboxymethyl cellulose; PAA, polyacrylic acid.

nZVI type	Particle size	N2-BET SSA (m2 g-1)	pH (1:10 w/v)	Polymer Mw (kg mol^{-1})	Zeta potential (mV)
nZVI	50-100nm	19.4[a]	7.53	--	-1.45[c]
CMC-nZVI	50-100nm	20.2	7.49	90[b]	-45.8[c]
PAA-nZVI	50-100nm	22.5[a]	11.0[a]	1.8[a]	-31.6[c]

[a]Data obtained from the instructions provided by the supplier (Nano Iron Ltd., Rajhrad, Czech Republic).

[b]Data obtained from instructions provided by the manufacturer (Sigma-Aldrich, Saint Louis, Missouri, USA).

[c]Data was from Raychoudhury et al. (2010).[5] Here it is reasonable to refer to this data as we used the same CMC and PAA materials and prepared the CMC-/PAA- coated nZVI using the same procedure.

Table S3. Concentrations of different microbes in the 2-mm thick soil surrounding the layer of different nZVI particles for different treatments after 56 days of exposure as revealed by phospholipid fatty acid (PLFA) analysis. Notes: CK, no nZVI in nylon layers; nZVI (bare nano zero-valent iron in nylon layers); CMC-nZVI (carboxymethyl-cellulose-coated nano zero-valent iron in nylon layers); PAA-nZVI (polyacrylic-acid-coated nano zero-valent iron in nylon layers). For two-way ANOVA, Radiation: γ-radiation treatment; nZVI: nano zero-valent iron (with/without different coatings) presence. ns, not significant; *P < 0.05; **P < 0.01. Different letters show significant difference based on Duncan multiple range test (P < 0.05).

Treatment		Total microbe (mmol kg^{-1})	Total bacteria (mmol kg^{-1})	Actinobacteria (mmol kg^{-1})	G^+ bacteria (mmol kg^{-1})	G^- bacteria (mmol kg^{-1})	Anaerobic microbe (mmol kg^{-1})	Total fungi (μmol kg^{-1})
Non-radiated	CK	0.58 ± 0.01^{ab}	0.34 ± 0.02^{ab}	0.03 ± 0.00^{a}	0.14 ± 0.01^{ab}	0.15 ± 0.01^{b}	0.10 ± 0.01^{b}	3.27 ± 0.60
	nZVI	0.54 ± 0.03^{abc}	0.33 ± 0.04^{ab}	0.02 ± 0.01^{abc}	0.15 ± 0.02^{a}	0.15 ± 0.01^{b}	0.09 ± 0.01^{b}	2.90 ± 0.35
	CMC-nZVI	0.52 ± 0.06^{abc}	0.32 ± 0.04^{abc}	0.03 ± 0.01^{ab}	0.14 ± 0.02^{ab}	0.14 ± 0.02^{b}	0.08 ± 0.01^{b}	2.73 ± 0.51
	PAA-nZVI	0.51 ± 0.01^{abc}	0.31 ± 0.01^{abc}	0.02 ± 0.01^{abc}	0.12 ± 0.01^{ab}	0.15 ± 0.00^{b}	0.08 ± 0.00^{b}	3.07 ± 0.35
γ-radiatied	CK	$0.49 \pm .03^{bc}$	0.29 ± 0.02^{bc}	0.02 ± 0.00^{bc}	0.12 ± 0.00^{b}	0.14 ± 0.02^{b}	0.08 ± 0.01^{b}	3.17 ± 0.59
	nZVI	0.62 ± 0.08^{a}	0.38 ± 0.05^{a}	0.02 ± 0.00^{bc}	0.13 ± 0.02^{ab}	0.22 ± 0.04^{a}	0.16 ± 0.03^{a}	3.10 ± 0.75
	CMC-nZVI	0.43 ± 0.02^{c}	0.24 ± 0.01^{c}	0.02 ± 0.00^{bc}	0.07 ± 0.01^{c}	0.15 ± 0.00^{b}	0.11 ± 0.01^{b}	3.80 ± 0.87
	PAA-nZVI	0.54 ± 0.15^{abc}	0.31 ± 0.09^{abc}	0.02 ± 0.01^{c}	0.06 ± 0.02^{c}	0.23 ± 0.07^{a}	0.17 ± 0.06^{a}	3.53 ± 1.37
Significance of								
	Radiation	ns	ns	**	**	**	**	ns
	nZVI	*	*	ns	**	*	*	ns
	Radiation × nZVI	ns	ns	ns	**	*	**	ns

Table S4. Dissimilarity analysis of bacterial and fungal community composition (Illumina data) in soils surrounding nZVI layers as affected by γ-radiation treatment. The analysis was done at phylum, class, genus and OTU levels.

Comparisons		ANOSIM		Adonis			MRPP		
		R	*P*	R2	F	*P*	Observed δ	Expected δ	*P*
Bacterial community	Phylum	1.000	0.001	0.899	195	0.001	0.073	0.216	0.001
	Class	1.000	0.001	0.861	136	0.001	0.110	0.295	0.001
	Genus	1.000	0.001	0.885	169	0.001	0.118	0.338	0.001
	OTU	0.891	0.001	0.490	21.2	0.001	0.428	0.594	0.001
Fungal community	Phylum	0.562	0.002	0.490	21.1	0.001	0.136	0.200	0.001
	Class	0.309	0.005	0.275	8.36	0.007	0.215	0.259	0.007
	Genus	0.376	0.002	0.274	8.31	0.006	0.297	0.352	0.004
	OTU	0.445	0.001	0.223	6.33	0.001	0.537	0.605	0.001

Table S5. Physico-chemical traits of the soils after different treatments after 1 day's incubation. Soil pH was detected by using soil:water=1:5, dissolved organic carbon (DOC) and soluble metal elements were extracted by 0.01 mol L^{-1} $CaCl_2$. Notes: nZVI (bare nano zero-valent iron in nylon layers); CMC-nZVI (carboxymethyl-cellulose-coated nano zero-valent iron in nylon layers); PAA-nZVI (polyacrylic-acid-coated nano zero-valent iron in nylon layers). For two-way ANOVA, Radiation: γ-radiation treatment; nZVI: nano zero-valent iron (with/without different coatings) presence. ns, not significant; **P* < 0.05; ***P* < 0.01. Different letters show significant difference based on Duncan multiple range test (*P* < 0.05).

Treatment		pH	EC (μS cm^{-1})	Eh (mV)	DOC (mg kg^{-1})	Al (mg kg^{-1})	Fe (mg kg^{-1})	Mn (mg kg^{-1})	Mg (mg kg^{-1})	K (mg kg^{-1})	Zn (mg kg^{-1})	Pb (mg kg^{-1})
Non radiated	CMC-nZVI	6.10± 0.15	58.7±6.43	318±21.8	219±39.4	1.25±0.80	1.25±0.80	55.0±2.02^{b}	56.3±3.67	116±12.3	320±8.59	1.32±0.12
	nZVI	6.06±0.01	45.7±1.46	300±14.6	161±19.4	0.53±0.27	0.53±0.20	53.1±0.87^{b}	59.6±0.93	120±8.02	332±0.56	1.20±0.06
	PAA-nZVI	6.12±0.01	59.7±4.04	305±2.89	159±13.9	0.53±0.38	0.53±0.25	60.2±13.1^{b}	60.1±1.47	123±6.07	325±16.9	1.13±0.25
γ radiated	CMC-nZVI	6.28±0.33	78.7±6.00	283±13.0	248±32.3	0.91±0.33	1.24±0.24	74.5±1.46^{a}	60.6±2.20	125±6.97	337±6.18	1.44±0.08
	nZVI	6.09±0.13	63.0±9.54	315±8.08	201±22.6	0.65±0.33	0.69±0.23	76.7±3.48^{a}	59.7±1.95	122±9.95	339±3.42	1.27±0.05
	PAA-nZVI	6.00±0.03	70.2±15.8	314±7.77	250±59.6	0.85±0.39	0.79±0.29	74.8±2.27^{a}	59.2±2.26	122±1.21	333±7.52	1.35±0.05
significance of												
	Radiation	ns	**	ns	ns	ns	ns	**	ns	ns	ns	ns
	nZVI	ns	ns	ns	ns	ns	ns	ns	ns	ns	ns	ns
	Radiation × nZVI	ns	ns	ns	ns	ns	ns	ns	ns	ns	ns	ns

Table S6. Physico-chemical traits of the soils after different treatments after 56 days' incubation. Soil pH was detected by using soil:water=1:5, dissolved organic carbon (DOC) and soluble metal elements were extracted by 0.01 mol L^{-1} $CaCl_2$. Notes: CK, no nZVI in nylon layers; nZVI (bare nano zero-valent iron in nylon layers); CMC-nZVI (carboxymethyl-cellulose-coated nano zero-valent iron in nylon layers); PAA-nZVI (polyacrylic-acid-coated nano zero-valent iron in nylon layers). For two-way ANOVA, Radiation: γ-radiation treatment; nZVI: nano zero-valent iron (with/without different coatings) presence. ns, not significant; *$P < 0.05$; **$P < 0.01$, ***$P < 0.001$. Different letters show significant difference based on Duncan multiple range test ($P < 0.05$).

Treatment		pH	EC (μS cm^{-1})	Eh (mV)	DOC (mg kg^{-1})	Al (mg kg^{-1})	Fe (mg kg^{-1})	Mn (mg kg^{-1})	Mg (mg kg^{-1})	K (mg kg^{-1})	Zn (mg kg^{-1})	Pb (mg kg^{-1})
Non radiated	CK	5.48±0.08^{b}	117±25.5^{bc}	349±4.36^{a}	130±15.3^{ab}	1.16±0.27^{a}	0.69±0.19	32.6±3.77^{b}	66.1±2.20^{a}	91.0±4.61^{e}	399±4.34^{ab}	2.35±0.10^{a}
	CMC-nZVI	5.67±0.06^{b}	163±21.6^{ab}	316±11.5^{bc}	115±20.2^{ab}	0.55±0.23^{ab}	0.53±0.16	11.8±0.71^{c}	57.4±1.30^{b}	106±2.43^{d}	382±4.17^{bc}	1.57±0.07^{b}
	nZVI	5.66±0.05^{b}	126±24.1^{bc}	341±30.4^{ab}	79.3±23.2^{b}	0.30±0.11^{b}	0.26±0.12	13.9±1.70^{c}	58.7±1.26^{b}	112±4.45^{bcd}	406±13.8^{a}	1.72±0.18^{b}
	PAA-nZVI	5.71±0.06^{b}	194±52.0^{a}	319±8.19^{bc}	90.4±20.9^{b}	0.29±0.21^{b}	0.38±0.20	14.4±2.68^{c}	60.6±0.64^{b}	110±2.94^{cd}	367±13.9^{c}	1.27±0.22^{c}
γ radiated	CK	6.11±0.22^{a}	63.0±13.9^{c}	306±25.2^{c}	111±13.0^{ab}	0.44±0.25^{b}	0.54±0.24	137±3.81^{a}	58.7±0.91^{b}	117±4.93^{abcd}	279±8.53^{d}	0.94±0.04^{d}
	CMC-nZVI	6.26±0.02^{a}	88.3±5.86^{c}	291±12.9^{c}	152±26.0^{a}	0.49±0.39^{ab}	0.55±0.29	128±4.48^{a}	59.8±1.56^{b}	126±6.56^{a}	280±6.20^{d}	0.90±0.08^{d}
	nZVI	6.30±0.04^{a}	72.3±1.35^{c}	288±25.5^{c}	145±18.3^{a}	0.31±0.23^{b}	0.38±0.20	134±3.35^{a}	57.1±0.38^{b}	118±3.82^{abc}	276±3.19^{d}	0.88±0.08^{d}
	PAA-nZVI	6.31±0.12^{a}	89.3±9.02^{c}	298±28.3^{c}	121±4.83^{ab}	0.47±0.36^{ab}	0.52±0.29	133±5.20^{a}	60.2±0.86^{b}	122±1.59^{ab}	261±1.36^{d}	0.83±0.05^{d}
significance of												
	Radiation	***	***	***	**	ns	ns	***	**	***	***	***
	nZVI	**	**	ns	ns	*	ns	***	***	***	***	***
	Radiation × nZVI	ns	ns	ns	**	*	ns	**	***	**	*	***

Table S7. ANOVA results of effects of radiation and nZVI type on bacterial genus abundance. Notes: Radiation: γ-radiation treatment; nZVI: nano zero-valent iron (with/without different coatings) presence. ns, not significant; *P < 0.05; **P < 0.01, ***P < 0.001.

Bacterial genus	Significance of		
	Radiation	nZVI	Radiation × nZVI
Massilia	***	*	ns
Bacillus	ns	*	**
Sphingomonas	***	ns	*
Phenylobacterium	***	ns	*
Rhodoplanes	***	ns	ns
Shewanella	***	***	**
Sediminibacterium	***	ns	ns
Rhizobium	***	***	***
Ramlibacter	***	ns	*
Leifsonia	***	***	***
Burkholderia	***	*	*
Methylobacterium	***	***	***
Cupriavidus	***	**	**
Enhydrobacter	***	*	*

Table S8. ANOVA results of effects of radiation and nZVI type on fungal genus abundance. Notes: Radiation: γ-radiation treatment; nZVI: nano zero-valent iron (with/without different coatings) presence. ns, not significant; *P < 0.05; **P < 0.01, ***P < 0.001.

Fungal genus	Significance of		
	Radiation	nZVI	Radiation × nZVI
Penicillium	*	**	ns
Mortierella	***	***	***
Solicoccozyma	***	***	***
Chrysosporium	***	ns	ns
Aspergillus	**	ns	**
Oidiodendron	ns	***	ns
Pseudogymnoascus	*	***	ns
Fusarium	ns	*	*
Humicola	***	**	**
Trichoderma	ns	ns	ns
Paecilomyces	ns	ns	ns
Phialemonium	*	ns	ns
Coniochaeta	ns	ns	ns
Thermomyces	**	**	**
Ascochyta	**	**	**
Rhodotorula	ns	ns	ns
Rhodosporidiobolus	ns	ns	ns

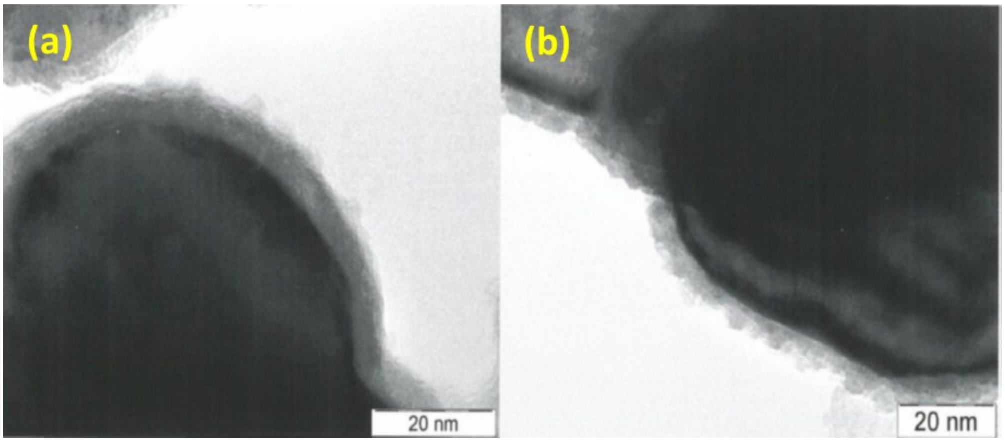

Figure S1. Transmission electron micrographs (TEM) of fresh nano zero-valent iron (nZVI) provided by Nano Iron Ltd. (Rajhrad, Czech Republic). TEM images (a) and (b) are from the manufacturer's instructions, showing the compact Fe oxide layer on the fresh nZVI particles (a) and eroded layer on the nZVI particles after activation (20% of nZVI products in 80% of water was mixed for 10 min, and then kept at room temperature for 48h to reach the highest activity of the nZVI particles) (b).

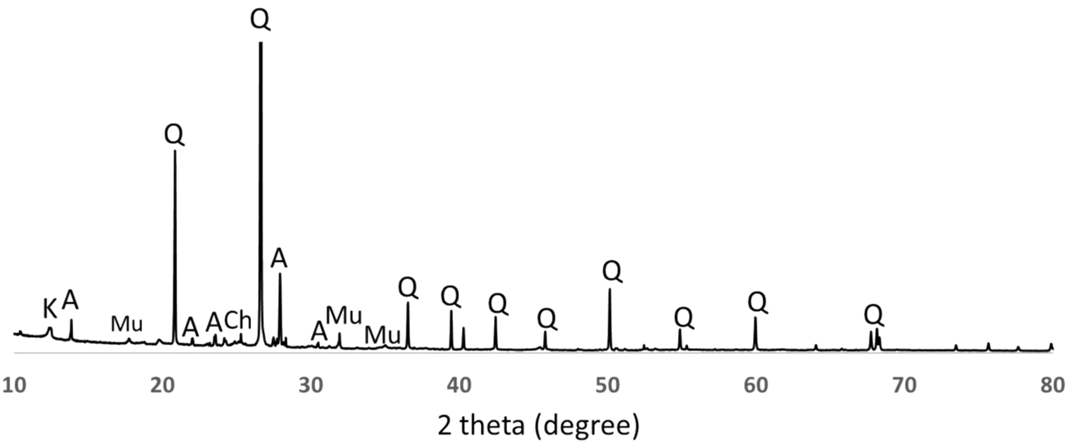

Figure S2. X ray diffraction (XRD) patterns of soils used for this study. Q: quartz (SiO_2); A: albite $Na(AlSi_3O_8)$; K: kaolinite ($Al_2Si_2O_5(OH)_4$); Ch: chamosite 1M ($(Mg_{5.036}Fe_{4.964})Al_{2.724}(Si_{5.70}Al_{2.30}O_{20})(OH)_{16}$); Mu: muscovite 2M1, ferrian ($K_{0.92}Na_{0.08}Al_{1.78}Fe_{0.22}Mg_{0.1}(Al_{0.83}Si_{3.17}O_{10})(OH)_{1.56}O_{0.25}F_{0.19}$).

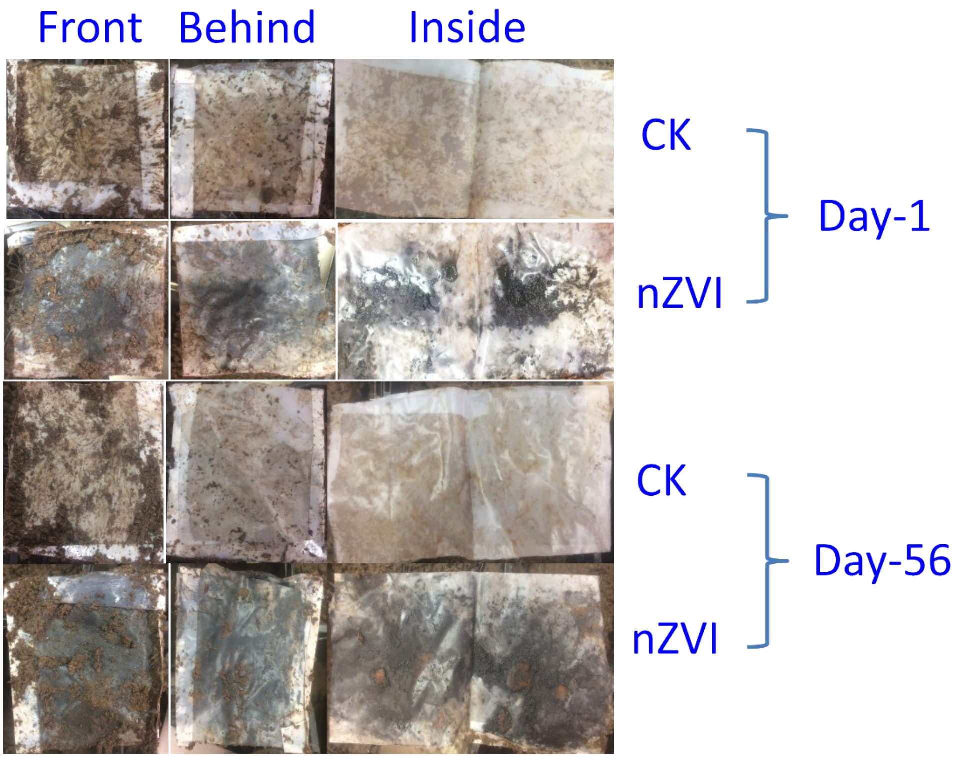

Figure S3. Photos showing nylon net with/without nZVI inside in the soils after 1- and 56-days' incubation. The photos indicate that there is no soil penetration into the nylon net in the control treatment (CK, without nZVI inside), while in the nylon net with nZVI inside, the nZVI aging products aggregated in the nylon bag.

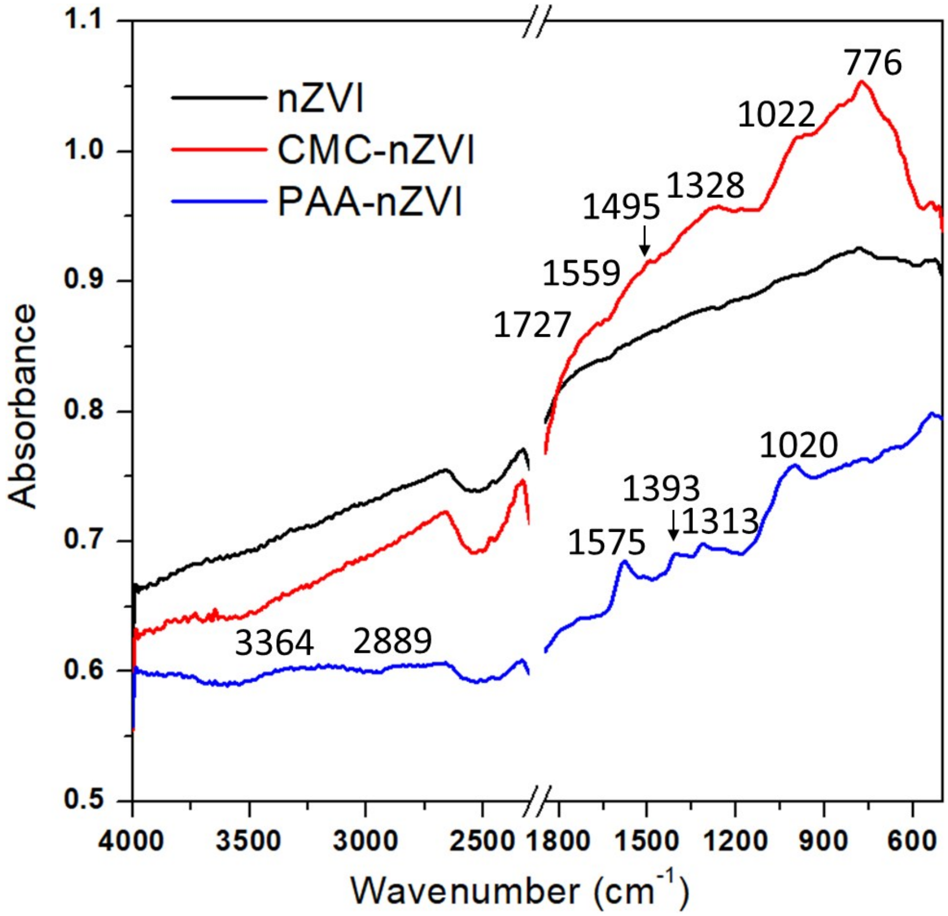

Figure S4. ATR-FTIR spectra of fresh nZVI of different type. Note: nZVI, bare nano zero-valent iron; CMC-nZVI, carboxymethyl cellulose coated nano zero-valent iron; PAA-nZVI, polyacrylic acid coated nano zero-valent iron.

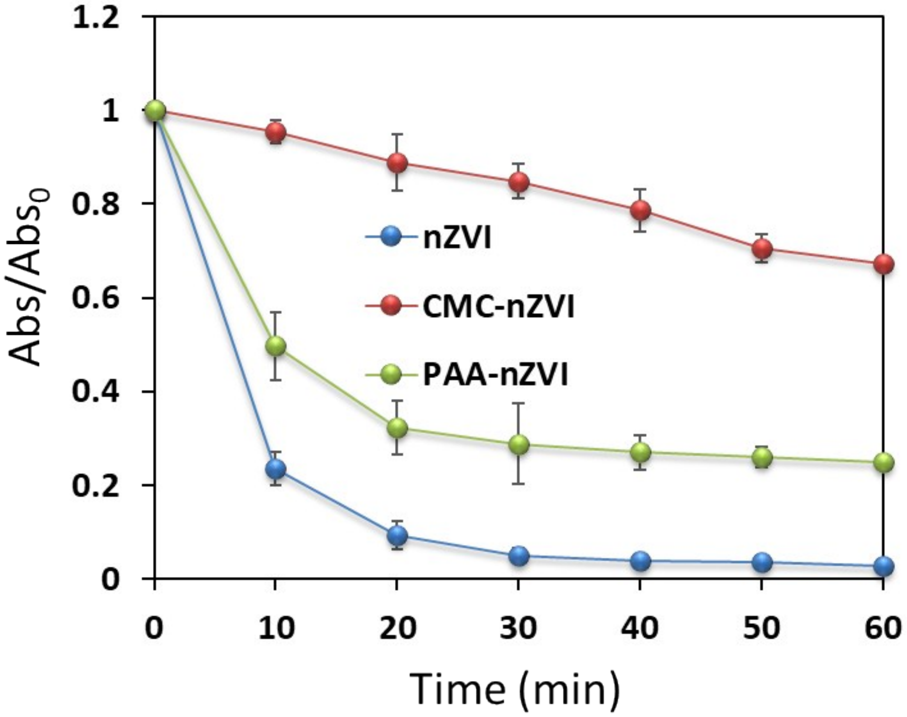

Figure S5. Changes in relative absorbance over time (0–60 min) in sedimentation tests with bare, CMC-coated (0.3% w/w), and PAA-coated (0.3% w/w) nZVI at a suspension concentration of 2.0% Fe (w/w). Note: the experiment was performed in triplicates (n=3); nZVI, nano zero-valent iron; CMC, carboxymethyl cellulose; PAA, polyacrylic acid.

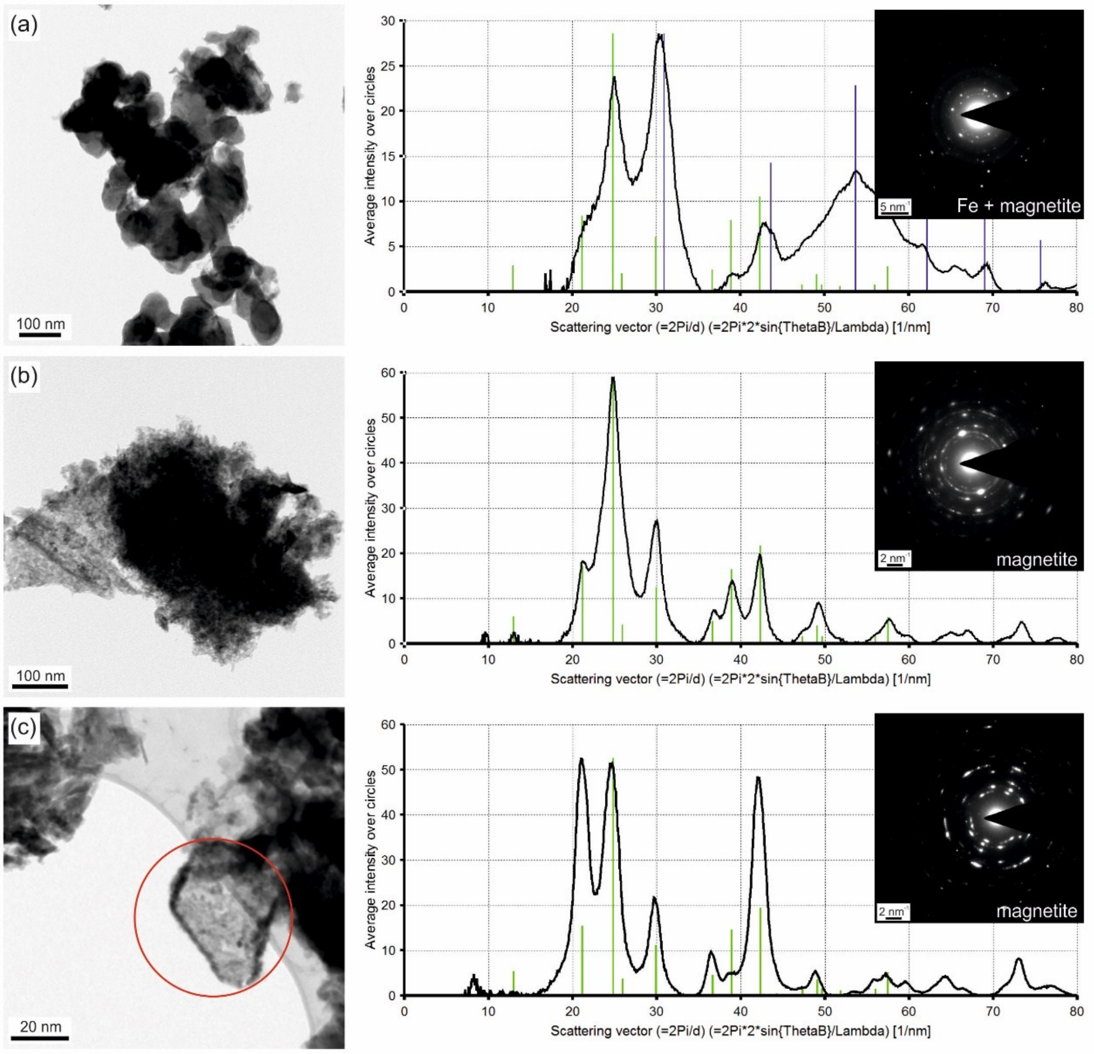

Figure S6. Transmission electron microscope (TEM) images and selected area electron diffraction (SAED) interpretation of bare nano zero-valent iron (nZVI) at day 0 (a) and after 56 days of aging in γ-radiated (b) and non-radiated soils (c).

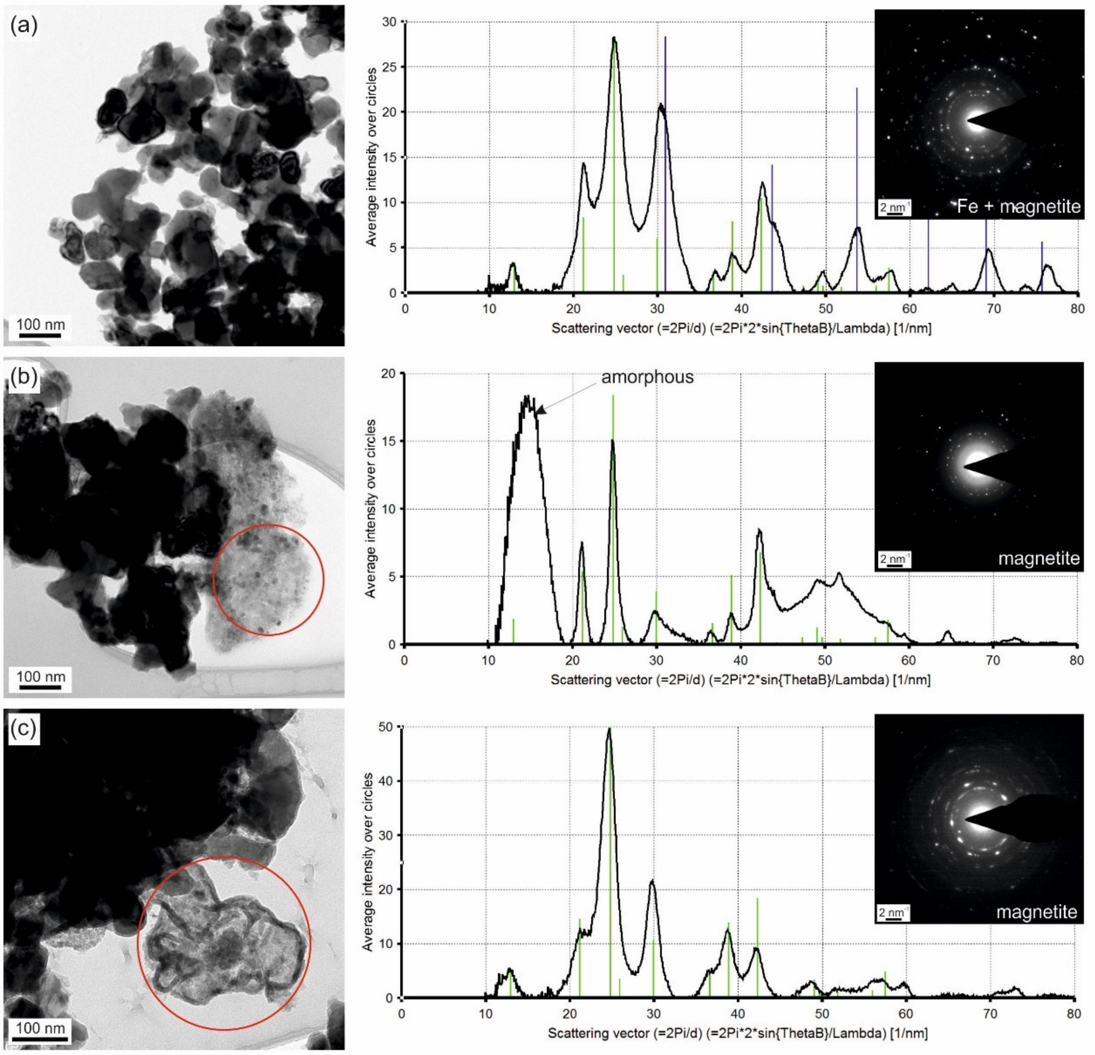

Figure S7. Transmission electron microscope (TEM) images and selected area electron diffraction (SAED) interpretation of carboxymethyl cellulose (CMC)-coated nano zero-valent iron (nZVI) at day 0 (a) and after 56 days of aging in γ-radiated (b) and non-radiated soils (c).

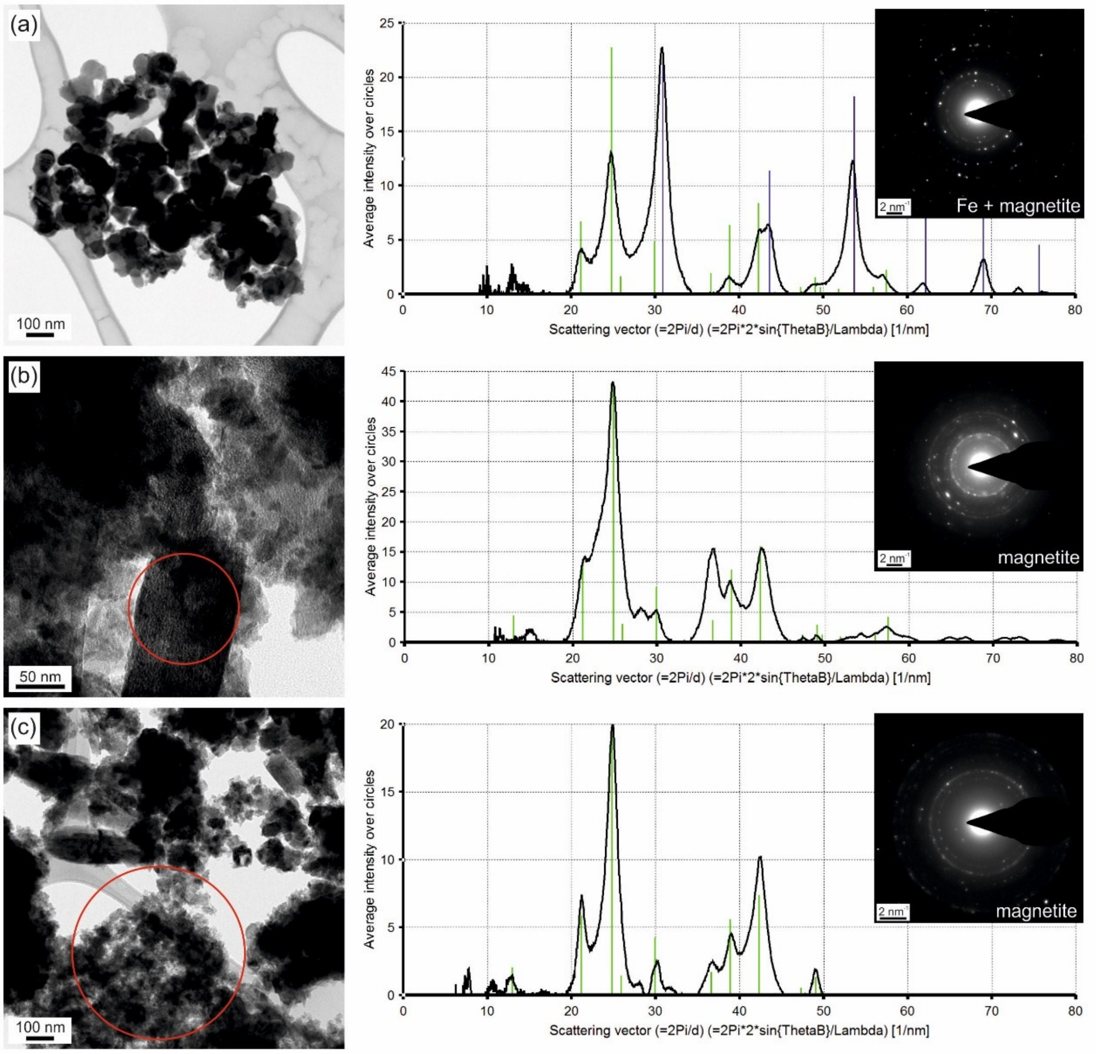

Figure S8. Transmission electron microscope (TEM) images and selected area electron diffraction (SAED) interpretation of polyacrylic acid (PAA)-coated nano zero-valent iron (nZVI) at day 0 (a) and after 56 days of aging in γ-radiated (b) and non-radiated soils (c).

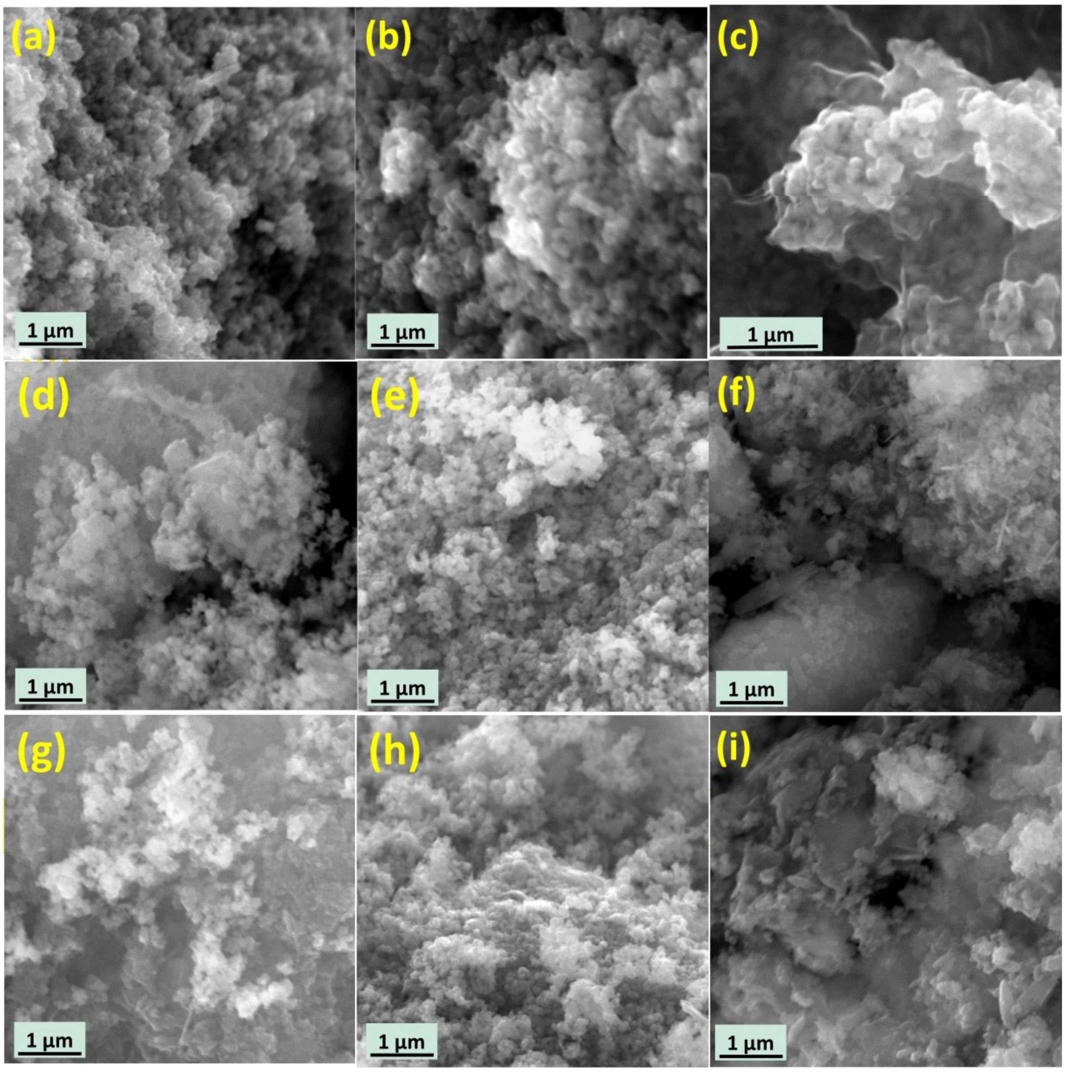

Figure S9. Scanning electron microscope (SEM) images showing fresh nano zero-valent iron (nZVI) and nZVI aging products after 56 days of cultivation in soils. Note: (a), (d), and (g) are bare nZVI; (b), (e), and (h) are CMC-coated nZVI; (c), (f), and (i) are PAA-coated nZVI. (a), (b), and (c), fresh nZVI particles; (d), (e), and (f), nZVI particles with γ-radiation treatment; (g), (h), and (i), nZVI particles with non-radiation treatment.

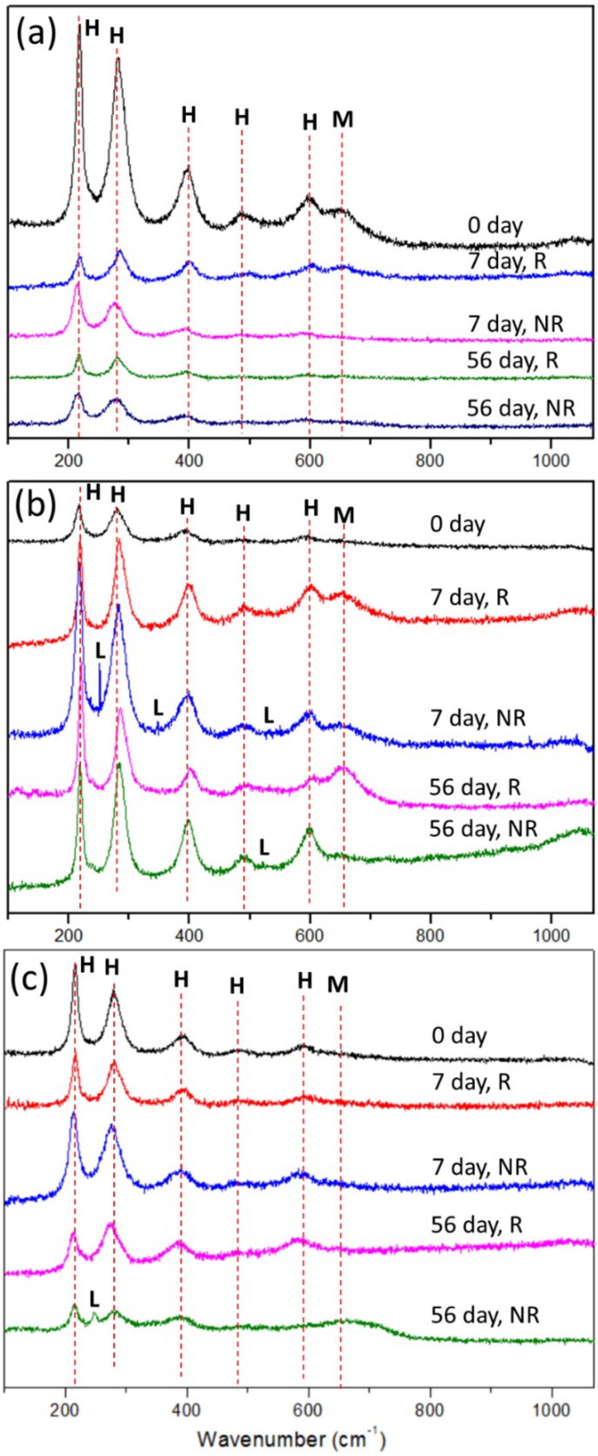

Figure S10. Raman spectra of nZVI and its aging products at different periods. (a) bare nZVI; (b) CMC-nZVI; (c) PAA-nZVI. Note: H: hematite; M: magnetite; L: lepidocrocite; G: goethite; R represents γ-radiated soil (altered soil microbial community); NR represents non-radiated soil (with original soil microbial community); nZVI, nano zero-valent iron; CMC, carboxymethyl cellulose; PAA, polyacrylic acid.

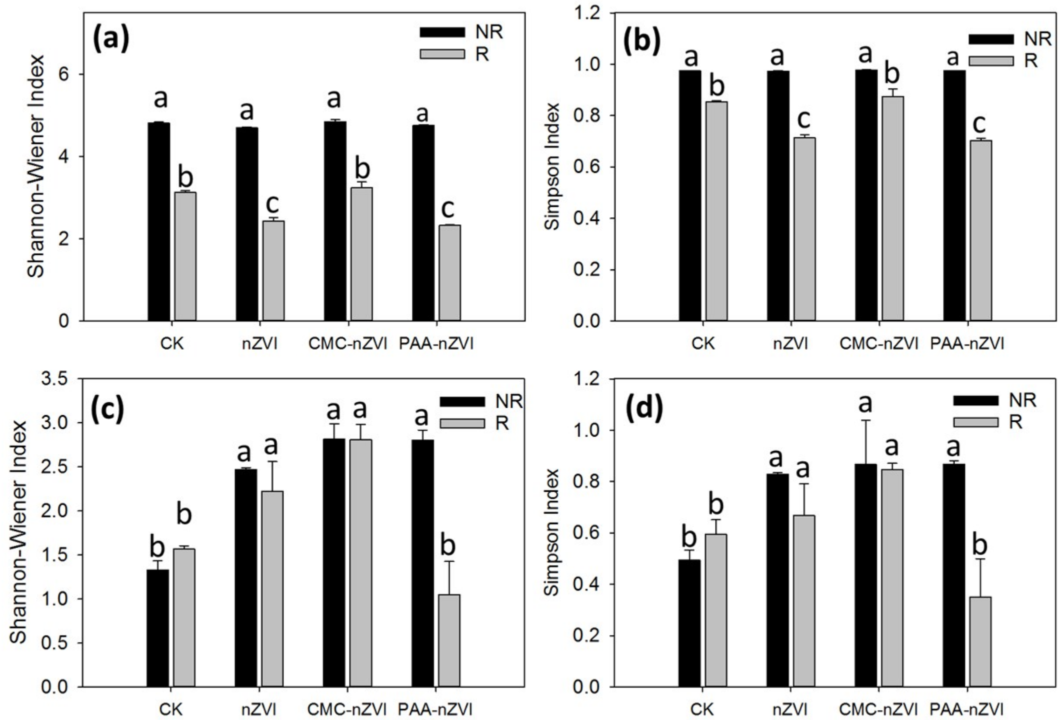

Figure S11. Bacterial (a, b) and fungal (c, d) diversity (based on Illumina data at OTU level) in the soil surrounding the layer of different nZVI particles (2 mm around the nZVI layer) with different treatments after 56 days of exposure. (a) and (c) are Shannon–Wiener Index, (b) and (d) are Simpson Index. Notes: CK, no nZVI in nylon layers; CMC-nZVI (CMC-coated nZVI in nylon layers); nZVI (bare nZVI in nylon layers); PAA-nZVI (PAA-coated nZVI in nylon layers); R represents γ-radiated soil; NR represents non-radiated soil. nZVI, nano zero-valent iron; CMC, carboxymethyl cellulose; PAA, polyacrylic acid. Different letters above columns show significant difference based on Duncan multiple range test ($P < 0.05$).

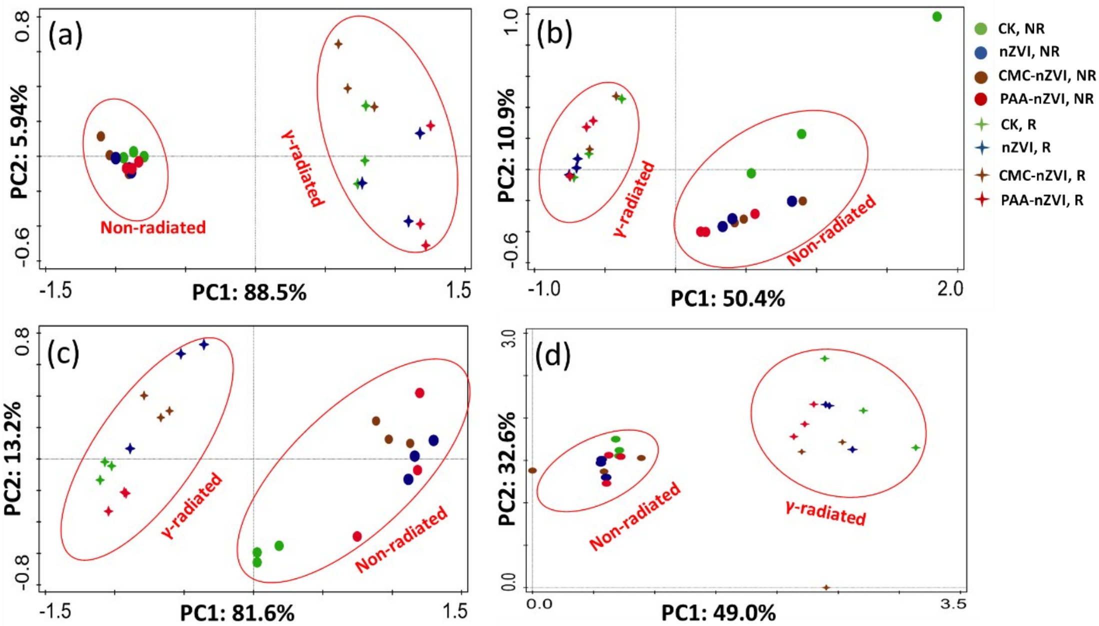

Figure S12. Multivariate analysis based on bacterial and fungal community information (Illumina data) at the phylum and OTU levels. (a) Principal component analysis (PCA) based on bacterial phylum level distribution, (b) PCA based on bacterial OTU level distribution, (c) PCA based on fungal phylum level distribution, and (d) PCA based on fungal OTU level information. Note: CK, NR represents no nZVI in nylon layers and no soil radiation; CMC-nZVI, NR represents CMC-coated nZVI in nylon layers without soil radiation; nZVI, NR represents bare nZVI in nylon layers without soil radiation; PAA-nZVI, NR represents PAA-coated nZVI in nylon layers without soil radiation; CK, R represents no nZVI in nylon layers with soil γ-radiation; CMC-nZVI, R represents CMC-coated nZVI in nylon layers with soil γ-radiation; nZVI, R represents bare nZVI in nylon layers with soil γ-radiation; PAA-nZVI, R represents PAA-coated nZVI in nylon layers with soil γ-radiation. nZVI, nano zero-valent iron; CMC, carboxymethyl cellulose; PAA, polyacrylic acid.

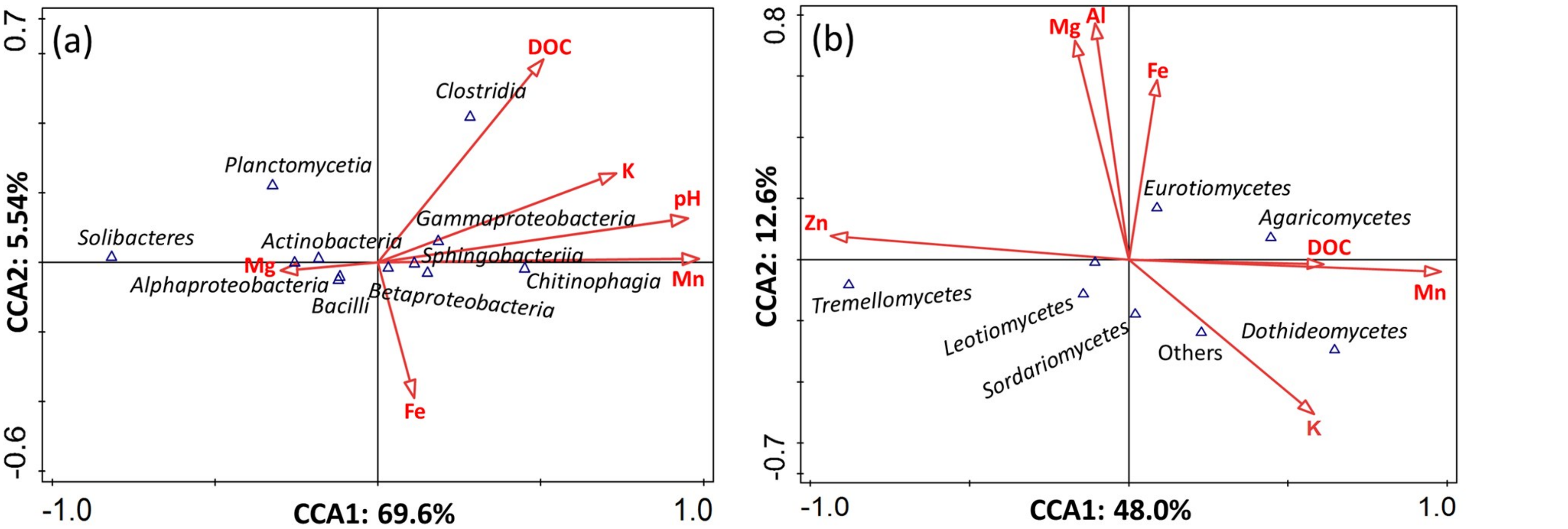

Figure S13. Ordination diagram from canonical correspondence analysis (CCA) analysis of bacterial (a) and fungal (b) community at class level (Illumina data) in soils surrounding nZVI layer with different treatments. The results showed that DOC, pH, $CaCl_2$ extractable K, Mn, K and Mg together explained 79.3% of the bacterial community at class level, within which DOC, pH and $CaCl_2$-extractable Mn were the dominant factors that interacts with bacterial community. $CaCl_2$-extractable Mn, Mg, Al, Fe, Zn, K and DOC together explained 72.2% of the variation of the fungal community at class level, within which $CaCl_2$ extractable Mn, Mg and K were the dominant factors that interact with fungal community.

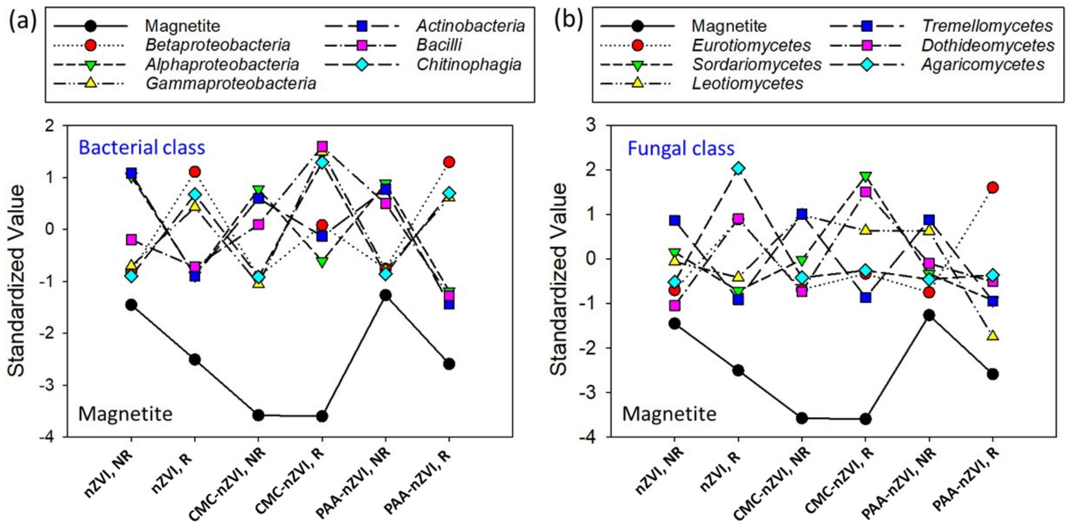

Figure S14. Changes of key bacterial class (a) and fungal class (b) abundance (mean value of three replicates, based on Illumina data) in the soils surrounding nZVI layers, in comparison with the trends of magnetite abundance (based on the result of quantification analysis of XRD spectra) in the nZVI aging products, from different treatments. The data used for the figure was standardized to make the value of different data types at the same level, and the standardized value of magnetite abundance was set to be 2.5 lower than the standardize microbial abundance value to separate material abundance with microbial abundance. Note: R represents γ-radiated soil; NR represents non-radiated soil. nZVI, nano zero-valent iron; CMC, carboxymethyl cellulose; PAA, polyacrylic acid.

References

1. J. L. Lábár, Consistent indexing of a (set of) single crystal SAED pattern (s) with the ProcessDiffraction program, Ultramicroscopy, 2005, 103, 237-249.
2. B. Lafuente, R.T. Downs, H. Yang and N. Stone, The power of databases: the RRUFF project, *In Highlights in Mineralogical Crystallography,* ed. T. Armbruster and R. M. Danisi, De Gruyter, Berlin, Germany, 2015, pp. 1-30.
3. S. Covino, T. Fabianová, Z. Křesinová, M. Čvančarová, E. Burianová, A. Filipová, J. Voříšková, P. Baldrian and T. Cajthaml, Polycyclic aromatic hydrocarbons degradation and microbial community shifts during co-composting of creosote-treated wood, Journal of Hazardous Materials, 2016, 301, 17-26.
4. S. Wu, M. Vosátka, K. Vogel-Mikus, A. Kavčič, M. Kelemen, L. Šepec, P. Pelicon, R. Skála, A. R. V. Powter and M. Teodoro, Nano zero-valent iron mediated metal (loid) uptake and translocation by arbuscular mycorrhizal symbioses, Environmental Science & Technology, 2018, 52 (14), 7640-7651.
5. T. Raychoudhury, G. Naja and S. Ghoshal, Assessment of transport of two polyelectrolyte-stabilized zero-valent iron nanoparticles in porous media, Journal of Contaminant Hydrology, 2010, 118, 143-151.